Multiscale Geometric Representation for Single Image Super-Resolution

S. H. Jagtap, M. M. Patil, S. D. Ruikar

Abstract - This paper presents comparative study of different single image SR algorithms and takes deep drive on a new approach to single-image super-resolution, based upon Multiscale Geometric Representations. Nowadays computational power of processors are increasing therefore, it has become feasible to use more robust and computationally complex algorithms that increase the resolution of images without distorting edges and contours. We present a novel image interpolation algorithm that uses the new contourlet transform to improve the regularity of object boundaries in the generated images. By using a simple wavelet-based linear interpolation scheme as our initial estimate, we use an iterative projection process based on two constraints to drive our solution towards an improved high-resolution image. This algorithm generates high-resolution images that are competitive or even superior in quality to images produced by other similar SR methods.

Keywords— Image super-resolution (SR), contourlet transform, geometric regularity, directional multi-resolution image.

I. INTRODUCTION

Super-Resolution (SR) is a technique to increase the resolution of an image or a sequence of images beyond the resolving power of the imaging system. The resolution of an image is defined as the amount of fine details that are visible. Nowadays Super-resolution image reconstruction is a active area of research, as it is capable of overcoming some resolution limitations of low-cost imaging sensors such as Cell phone cameras. This allows better utilization of the growing capability of high-resolution displays such as high-definition LCDs. Such resolution enhancing technology is important in medical imaging and satellite imaging where diagnosis or analysis from low-quality images can be extremely difficult. Conventional approaches to generating a super-resolution image normally require as input multiple low-resolution images of the same scene, which are aligned with sub-pixel accuracy [5]. The SR task is cast as the inverse problem of recovering the original high-resolution image by fusing the low-resolution images, based on reasonable assumptions or prior knowledge about the observation model that maps the high-resolution image to the low-resolution ones. The fundamental reconstruction constraint for SR is that the recovered image, after applying the same generation model, should reproduce the observed low-resolution images.

Manuscript received March 31, 2012

Mr. S. H. Jagtap, Department of Electronic and Telecommunication Engineering, Pune University, Sinhgad Academy of Engineering Kondhwa (Bk), Pune-411048, Dist-Pune, Maharashtra, India.

Prof. M. M. Patil, Department of Electronic and Telecommunication Engineering, Pune University, Sinhgad Academy of Engineering Kondhwa (Bk), Pune-411048, Dist-Pune, Maharashtra, India.

Prof. S. D. Ruikar, Department of Electronic and Telecommunication Engineering, Pune University, Sinhgad Academy of Engineering Kondhwa (Bk), Pune-411048, Dist-Pune, Maharashtra, India.

However, SR image reconstruction is generally a severely ill-posed problem because of the insufficient number of low-resolution images, ill-conditioned registration and unknown blurring operators and the solution from the reconstruction constraint is not unique [2], [7], [13], [24], [27]. Various regularization methods have been proposed to further stabilize the inversion of this ill-posed problem, such as [5], [23]. However, the performance of these reconstruction-based SR algorithms degrades rapidly when the desired magnification factor is large or the number of available input images is small. Another SR approach is based upon interpolation. While simple interpolation methods such as Nearest Neighbour interpolation, Bilinear interpolation, Bicubic interpolation and Cubic spline interpolation tend to generate overly smooth images with ringing and jagged artefacts, interpolation by exploiting the natural image priors will generally produce more favourable results [6].

A third category of SR approach is based upon machine learning techniques [2], [3], [7], [19], [24], [27], which attempt to capture the co-occurrence prior between low-resolution and high-resolution image patches. Learning strategy that applies to generic images where the low-resolution to high-resolution prediction is learned via different methods. But these methods typically require enormous databases of millions of high-resolution and low-resolution patch pairs, and are therefore computationally intensive. The most common methods used in practice, such as bilinear and bicubic interpolation, require only a small amount of computation. However, because they are based on an oversimplified slow varying image model, these simple methods often produce images with various problems along object boundaries, including aliasing, blurring, and zigzagging edges. Various interpolation algorithms have been proposed to reduce edge artifacts, aiming at obtaining images with regularity (i.e. smoothness) along edges. In one of the earliest papers on the subject, Jensen and Anastassiou [22] propose to estimate the orientation of each edge in the image by using projections onto an orthonormal basis and the interpolation process is modified to avoid interpolating across the edge. Allebach and Wong [23] propose to use an estimate of the high-resolution edge map to iteratively correct the interpolated pixels. Another low-cost, yet quite eff ective method called data dependent triangulation [24] performs interpolation by dividing every four-pixel square into two triangles and restricts interpolation to within the triangles. Instead of explicitly estimating edges, Li and Orchard [25] propose a statistical estimation method that tunes interpolation coefficients according to local edge structures. While this method produces superior results,

its computational complexity is prohibitive due to the large window size used to estimate local covariances. Improved interpolation methods have also been cast as a non-linear PDE problem, [26] where the algorithm attempts to satisfy smoothness and orientation constraints. Recently, methods have been proposed which perform interpolation in a transform (e.g. wavelet) domain. [27], [28] These algorithms assume the low-resolution image to be the lowpass output of the wavelet transform and utilize dependence across wavelet scales to predict the "missing" coefficients in the more detailed scales. In this paper, we propose a novel image interpolation algorithm based on the new contourlet transform, 8 which provides an efficient multiscale geometric representation for natural images. By enforcing a sparsity constraint on the coefficients of the contourlet transform, we provide an efficient mechanism that helps improve the regularity along edges in the resulting images. Furthermore, to satisfy the observation constraint provided by the given low-resolution image, we employ an iterative projection procedure in the wavelet domain, originally proposed by Guleryuz. [29].

II. METHODOLOGY

1) Interpolation Methods:

Interpolation is the process used to estimate an image value at a location in between image pixels. When we enlarge an image, the output image contains more pixels than the original image [6]. Interpolation methods determine the value for an interpolated pixel by finding the point in the input image that corresponds to a pixel in the output image and then calculating the value of the output pixel by computing a weighted average of some set of pixels in the vicinity of the point. The weightings are based on the distance each pixel is from the point. When you reduce the size of an image, you lose some of the original pixels because there are fewer pixels in the output image and this can cause aliasing. Aliasing that occurs as a result of size reduction normally appears as "stair-step" patterns (especially in high-contrast images), or as moire (ripple-effect) patterns in the output image. Antialiasing is used to limit the impact of aliasing on the output image for all interpolation types except nearest neighbor. There are mainly three algorithms used in interpolation to determine the values for the additional pixels which is Nearest neighbor interpolation, Bilinear interpolation and Bicubic interpolation.

First we will see the Nearest neighbor interpolation method. In the nearest neighbor interpolation, the block uses the value of nearby translated pixel values for the output pixel values. This Nearest neighbor interpolation shows check board effect as zooming factor increases. To smooth the image Bilinear interpolation come in the picture. In the Bilinear interpolation the block uses the weighted average of two translated pixel values for each output pixel value.

In the Bilinear interpolation output image is with aliasing effect, to reduce this antialiasing is used. But there is still problem as zooming factor increases. To solve this instead of using two pixel and linearly interpolate it, taking the weighted average of four translated pixel values for each output pixel value give better result. This method is called Bicubic interpolation.

2) Machine Learning Methods:

There are few methods in this category like [1]. But recently sparse representation is applied in different image processing areas such as denoising, restoration, super-resolution etc for improving on the performance [2], [3], [4]. The Multiscale Geometric Representation for Single Image Super-Resolution method is having main parts as,

A. THE NEW CONTOURLET TRANSFORM

The contourlet transform was proposed by Do and Vetterli [10] as a directional multi-resolution transform that can efficiently capture and represent smooth object boundaries in natural images. In this paper, we employ a new version of the contourlet transform, recently proposed by Lu and Do[8]. As an improvement over the original version, the basis images from the new transform are sharply localized in the frequency domain and exhibit smoothness along their main ridges in the spatial domain. In practice, this improved regularity of basis images helps reduce the artifacts in processed images, consequently making the new contourlet transform a more favorable choice for various image processing applications.

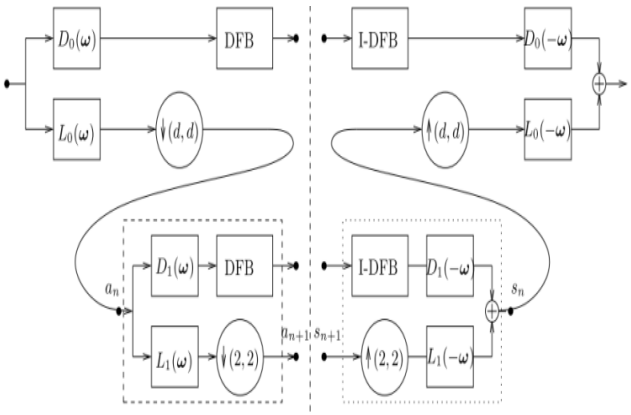

Fig 1. The block diagram of the new contourlet transform.

The directional filter banks (DFB) are attached to the highpass subbands of the multiscale pyramid at each level.

We show in Figure 1 the construction of the new contourlet transform. We use the directional filter banks (denoted by DFB and I-DFB for the analysis and synthesis parts, respectively) to achieve directional decomposition. Instead of using the Laplacian pyramid as in the original contourlet transform, we employ a new pyramid structure for the multiscale decomposition, which is conceptually similar to the one used in the steerable pyramid.

In Figure 1, we use Li(ω) (i = 0, 1) to represent the lowpass filters and Di(ω) (i = 0, 1) to represent the highpass filters in the multiscale decomposition, with $\omega \stackrel{\text{def}}{=} (\omega 1 , \omega 2)$. The DFB is attached to the highpass branch at the finest scale and bandpass branches at all coarser scales. The lowpass filter L0(ω) in the first level is downsampled by d along each dimension, with d being a number chosen from 1 and 2, and the lowpass filter L1(ω) in the second level is downsampled by (2, 2).

To have more levels of decomposition, we can recursively insert at point a n+1 a copy of the diagram contents enclosed by the dashed rectangle in the analysis part, and at point s n+1 a copy of the diagram contents enclosed by the dotted rectangle in the synthesis part.

As an important diff erence from the Laplacian pyramid used in the original contourlet transform, the new multiscale pyramid shown in Figure 1 can employ a diff erent set of lowpass and highpass filters for the first level and all other levels. This turns out to be a crucial step in reducing the frequency-domain aliasing of the DFB. We leave the detailed explanation for this issue as well as the specification of the filters Li(ω) and Di(ω) to reference [29].

B. INTERPOLATION BY ITERATING CONSTRAINTS

Main Ideas: We look to design an algorithm that will upsample a given low-resolution image (by factor of 2 n with n = 1, 2, . . .,for the sake of simplicity) that will improve the quality of interpolation in edge regions of the image. Like several papers than perform interpolation in the transform domain, we assume our low-resolution image to be the lowpass output of an n-level wavelet transform applied to the ground truth high-resolution image (to which we do not have access). The main idea of our algorithm is to alternately enforce two constraints, which is similar to the technique proposed in reference[29]. The first constraint comes from the assumption that the given low-resolution image is the downsampled output of the lowpass anti-aliasing filter in a wavelet transform. This observation constraint can be enforced by requiring the high-resolution image to have our given low-resolution image as its lowpass output of the wavelet transform. The second constraint is based on a model for natural images. Since the contourlet transform described in last section provides us with a sparse image representation well-suited to preserving contours and edges, we assume that the unknown high-resolution image should be sparse in the contourlet transform domain. As shown in Sparsity Constraint, we enforce this constraint through a hard-thresholding of the contourlet coefficients.

Observation Constraint: Figure 2 illustrates the observation constraint, in which we assume the given low-resolution image, denoted by xL , is the lowpass subband of an n-level wavelet transform of the unknown high-resolution image x, while all the coefficients in the highpass subbands have been discarded. As a simple way to get an estimate x̂0 of the high-resolution image, we can take the inverse wavelet transform by keeping xL as the lowpass band and zeropadding all highpass subbands. It has been observed by several authors that this simple scheme often outperforms other more sophisticated interpolation methods, which do not take into account the anti-aliasing operation in the image generation process.

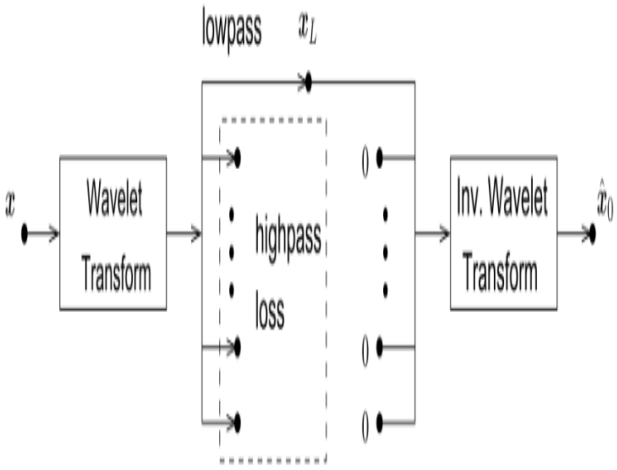

Fig 2. The observation model.

We assume the given low-resolution image xL is the lowpass subband of a wavelet transform applying on the unknown high-resolution image x. A simple estimation of the high-resolution image, denoted by x̂0, can be obtained by an inverse wavelet transform, which uses xL as the lowpass and zero coefficients for all highpass subbands.

Note that the set of all images whose lowpass wavelet subbands are equal to the given low-resolution image xL forms a linear variety. Consequently, for any given image y, we can calculate the best approximation (in L2 norm) to y, subject to our observation constraint, through orthogonal projection. Let W and W−1 represent the forward and inverse wavelet transforms, respectively; denote P as the diagonal projection matrix of 1's and 0's that keeps the lowpass wavelet coefficients and zeros out the high frequency subband coefficients, and let $P^{\perp} = I - P$. If we use orthonormal wavelet transforms, then the projection of any image y onto the constraint set can be calculated by

$$\hat{y} = W^{-1}(P^{\perp} W y + PW \hat{x}0) \quad (1)$$

where x̂0 is the estimation of the high-resolution image obtained as in Figure 2.

Sparsity Constraint: The contourlet transform provides us with a sparse image representation (i.e. there are many more insignificant coefficients than significant ones), and these coefficients well represent the edge regions of the image. Note that there can be several diff erent ways to enforce the sparseness constraint (e.g. see the pursuit schemes described in reference 16). For the sake of simplicity, we choose to use a direct hard-thresholding scheme in our proposed algorithm.

Intuitively, we view our estimate to the high-resolution image as a noisy version of the true image. Enforcing our sparsity constraint works to denoise the estimation of the interpolated signal while retaining the important coefficients near edges. Denote C and C−1 as the forward and inverse contourlet transforms, respectively; DT as the diagonal matrix that, given some threshold value T , zeros out insignificant coefficients in the coefficient vector whose absolute values are smaller than T;

$\hat{x}$ the noisy high-resolution image; and $\check{x}$ the denoised high-resolution image. The sparseness constraint by hardthresholding can be written as, $\check{x} = C^{-1}DT\ C\hat{x}$ (2)

Iterative Contourlet-Based Image Interpolation: We show in Figure 3 the block diagram of the proposed iterative contourlet-based image interpolation scheme,

Which can be summarized as follows:

1. We start our algorithm by taking x_0 , obtained by the simple wavelet interpolation shown in Figure 3, as the initial estimate of the high-resolution image.

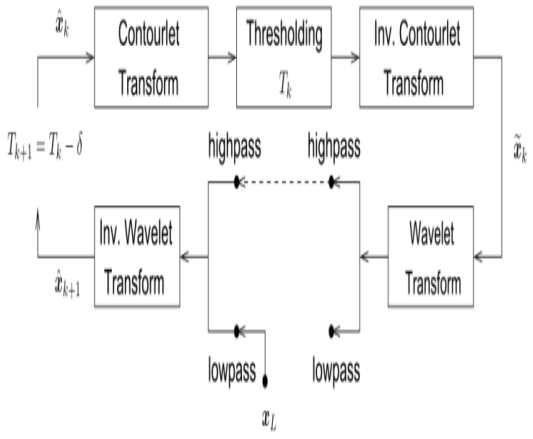

Fig 3. Block diagram of the proposed contourlet-based interpolation algorithm.

2. We then attempt to improve the quality of interpolation, particularly in regions containing edges and contours, by iteratively enforcing the observation constraint as well as the sparseness constraint. Let $\check{x}k$ represent the estimate at the k^{th} step. By combining (1) and (2), the new estimate $\check{x}_{k+1}$ can then be obtained by $\check{x}_{k+1} = W^{-1}(P^{\perp}WC^{-1}D_{Tk}\ C\check{x}_k + P\ W\check{x}_0)$.
3. Following the same principle of the sparseness-based image recovery algorithm proposed by Guleryuz, [29] we gradually decrease the threshold value T_k by a small amount δ in each iteration, i.e., $T_{k+1} = T_{k-\delta}$. This has been shown to be effective in circumventing the nonconvexity of the sparseness constraint.
4. Return to step 2 and keep iterating, until the generated images converge or a predetermined maximum iteration number has been reached.

III. RESULTS

In this section, we first demonstrate the SR results obtained by applying the previously mentioned methods and our method on different images. Then we show PSNRs and RMSEs of all SR methods.

Fig.4 (a) **Fig.4 (b)** **Fig.4 (c)** **Fig.4 (d)** **Fig.4 (e)** **Fig.4 (f)**

Fig. 4 shows results for Girl image.

Fig.4 (a) is down-sampled version of original image. Fig.4 (b) is High-Resolution image obtained from Nearest Neighbour Interpolation method. Fig.4 (c) is High-Resolution image obtained from Bilinear Interpolation method. Fig.4 (d) is High-Resolution image obtained from Cubic Spline Interpolation method and Fig.4 (e) is High-Resolution image obtained from MGR method and Fig.4 (f) is the original High-resolution image.

Fig.5 (a) **Fig.5 (b)** **Fig.5 (c)** **Fig.5 (d)** **Fig.5 (e)** **Fig.5 (f)**

Fig. 5 shows results for Flower image.

Published By:
Blue Eyes Intelligence Engineering
& Sciences Publication

Fig.5 (a) is down-sampled version of original image. Fig.5 (b) is High-Resolution image obtained from Nearest Neighbour Interpolation method. Fig.5 (c) is High-Resolution image obtained from Bilinear Interpolation method. Fig.5 (d) is High-Resolution image obtained from Cubic Spline Interpolation method and Fig.5 (e) is High-Resolution image obtained from MGR method and Fig.5 (f) is the original High-resolution image.

Fig.6 (a) **Fig.6 (b)** **Fig.6 (c)** **Fig.6 (d)** **Fig.6 (e)** **Fig.6 (f)**

Fig. 6 shows results for Bird image.

Fig.6 (a) is down-sampled version of original image. Fig.6 (b) is High-Resolution image obtained from Nearest Neighbour Interpolation method. Fig.6 (c) is High-Resolution image obtained from Bilinear Interpolation method. Fig.6 (d) is High-Resolution image obtained from Cubic Spline Interpolation method and Fig.6 (e) is High-Resolution image obtained from MGR method and Fig.6 (f) is the original High-resolution image.

Table 1: PSNRs of reconstructed images using different methods.

	Nearest Neighbour Interpolation	Bilinear Interpolation	Cubic Spline Interpolation	MGR SR
Lip Image	25.9098	26.5706	27.7517	29.1739
Fruit Image	26.9991	28.0214	29.3921	30.5472
Bird Image	25.5902	26.3417	27.5374	27.9257

Table 2: RMSEs of reconstructed images using different methods.

	Nearest Neighbour Interpolation	Bilinear Interpolation	Cubic Spline Interpolation	MGR SR
Girl Image	12.9137	11.9677	10.4461	8.8684
Flower Image	11.3916	10.1268	8.6483	7.5715
Bird Image	13.3977	12.2873	10.7071	10.2389

IV. CONCLUSIONS

In this paper, we have presented a novel image interpolation algorithm using the new contourlet transform. Our algorithm improves the regularity along edges in the interpolated image by treating each successive approximation to the high-resolution image as a noisy approximation and subsequently enforcing a sparsity constraint on the contourlet coefficients. Based on the given low-resolution image, we also enforce an observation constraint in the wavelet domain. By iterating this procedure and alternating between constraints, our algorithm converges towards an improved high-resolution image. We have shown improvement over simple wavelet based interpolation on a subjective scale, and in many cases with an improvement in PSNR. We expect to further reduce the computational complexity of our algorithm with future work, as we try to improve its rate of convergence.

REFERENCES

1. Jianchao Yang, John Wright, Thomas S. Huang, Yi Ma "Image Super-Resolution Via Sparse Representation" in IEEE transactions on image processing, VOL. 19, NO. 11, NOVEMBER 2010.
2. J. Yang, J. Wright, T. Huang, and Y. Ma "Image super-resolutions sparse representation of raw image patches" in Proc. IEEE Conf.Comput. Vis. Pattern Recognit., 2008, pp. 1–8.
3. Qi Pan, Chengying Gao, Ning Liu, Jiwu Zhu "Single Frame Image Super-resolution Based on Sparse Geometric Similarity" Journal of Information & Computational Science 7: 3 (2010) 799–805
4. Roman Zeyde, Michael Elad and Matan Protter "On Single Image Scale-Up using Sparse-Representations" The Computer Science Department Technion – Israel Institute of Technology – Haifa 32000.
5. S. Farsiu, M. D. Robinson, M. Elad, and P. Milanfar, "Fast and robust multiframe super-resolution" IEEE Trans. Image Process., vol. 13, no.10,pp. Oct.2004.
6. H. S. Hou and H. C. Andrews, "Cubic spline for image interpolation and digital filtering" IEEE Trans. Signal Process., vol. 26, no. 6, pp. 508–517, Dec. 1978.

7. J. Sun, Z. Xu, and H. Shum, "Image super-resolution using gradient profile prior" in Proc. IEEE Conf. Comput. Vis. Pattern Recognit., 2008, pp. 1–8.
8. Lyndsey C. Pickup "Machine Learning in Multi-frame Image Super-resolution" Robotics Research Group Department of Engineering Science University of Oxford, Michaelmas Term, 2007
9. M. E. Tipping and C. M. Bishop, "Bayesian image super-resolution" in Proc. Adv. Neural Inf. Process. Syst. 16, 2003, pp. 1303–1310.
10. S. Baker and T. Kanade, "Limits on super-resolution and how to break them" IEEE Trans. Pattern Anal. Mach. Intell., vol. 24, no. 9, pp. 1167–1183, Sep. 2002.
11. S. Dai, M. Han, W. Xu, Y. Wu, and Y. Gong, "Soft edge smoothness prior for alpha channel super resolution" in Proc. IEEE Conf. Comput. Vis. Pattern Class., 2007, pp. 1–8.
12. W. T. Freeman, E. C. Pasztor, and O. T. Carmichael, "Learning low level vision" Int. J. Comput. Vis., vol. 40, no. 1, pp. 25–47, 2000.
13. J. Sun, N. N. Zheng, H. Tao, and H. Shum, "Image hallucination with primal sketch priors" in Proc. IEEE Conf. Comput. Vis. Pattern Recognit., 2003, vol. 2, pp. 729–736.
14. S. T. Roweis and L. K. Saul, "Nonlinear dimensionality reduction by locally linear embedding" Science, vol. 290, no. 5500, pp. 2323–2326, 2000.
15. D. L. Donoho, "Compressed sensing" IEEE Trans. Inf. Theory, vol. 52, no. 4, pp. 1289–1306, Apr. 2006.
16. H. Rauhut, K. Schnass, and P. Vandergheynst, "Compressed sensing and redundant dictionaries" IEEE Trans. Inf. Theory, vol. 54, no. 5, May 2008.
17. M. Elad and M. Aharon, "Image denoising via sparse and redundant representations over learned dictionaries" IEEE Trans. Image Process., vol. 15, no. 12, pp. 3736–3745, Dec. 2006.
18. J. Mairal, G. Sapiro, and M. Elad, "Learning multiscale sparse representations for image and video restoration" Multiscale Model. Sim., vol. 7, pp. 214–241, 2008.
19. M. Aharon, M. Elad, and A. Bruckstein, "K-svd: An algorithm for designing overcomplete dictionaries for sparse representation" IEEE Trans. Signal Process., vol. 54, no. 11, pp. 4311–4322, Nov. 2006.
20. H. Lee, A. Battle, R. Raina, and A. Y. Ng, "Efficient sparse coding algorithms" in Proc. Adv. Neural Inf. Process. Syst., 2007, pp. 801–808.
21. Nickolaus Mueller, Yue Lu and Minh N. Do, "Image Interpolation Using Multiscale Geometric Representations" Department of Electrical and Computer Engineering University of Illinois at Urbana-Champaign.
22. K. Jensen and D. Anastassiou, "Subpixel edge localization and the interpolation of still images," IEEE Trans. Image Proc. 4, pp. 285–295, March 1995.
23. J. Allebach and P. W. Wong, "Edge-Directed interpolation," in Proc. IEEE Int. Conf. on Image Proc.,1996.
24. D. Su and P. Willis, "Image interpolation by pixel level data-dependent triangulation," Computer Graphics Forum 23, pp. 189–201, June 2004.
25. X. Li and M. T. Orchard, "New edge-directed interpolation," IEEE Trans. Image Proc. 10, pp. 1521–1527, October 2001.
26. H. Jiang and C. Moloney, "A new direction adaptive scheme for image interpolation," in Proc. IEEE Int. Conf. on Image Proc., pp. 369–372, 2002.
27. W. K. Carey, D. B. Chang, and S. S. Hermami, "Regularity-preserving image interpolation," IEEE Trans. Image Proc. 8, pp. 1293–1297, September 1999.
28. D. D. Muresan and T. W. Parks, "Prediction of image detail," in Proc. IEEE Int. Conf. on Image Proc., pp. 323–326, 2000.
29. O. G. Guleryuz, "Nonlinear approximation based image recovery using adaptive sparse reconstructions and iterated denoising: Part I - theory," IEEE Trans. Image Proc. 15, pp. 539–554, March 2006.